Title	Chemotactic Patterns in Biological Systems (Interfaces, Pulses and Waves in Nonlinear Dissipative Systems : RIMS Project 2000 "Reaction-diffusion systems : theory and applications")
Author(s)	Nomura, Atsushi
Citation	数理解析研究所講究録 (2001), 1191: 53-65
Issue Date	2001-02
URL	http://hdl.handle.net/2433/64753
Right	
Type	Departmental Bulletin Paper
Textversion	publisher

数理解析研究所講究録
1191 巻 2001 年 53-65

Chemotactic Patterns in Biological Systems

山口県立大学国際文化学部　野村厚志（Atsushi Nomura）
Faculty of International Studies, Yamaguchi Prefectural University.

1. Introduction

The *Dictyostelium* discoideum, a kind of slime mold, has a life cycle consisting of a vegetative stage and an animal stage. In the early vegetative stage, particular cells live independently under the rich food condition. However, once that their environmental condition becomes starvation, cells aggregate in the following way. First, some of vegetative cells begin to secrete the messenger molecule called "cAMP". Cells are attracted by a cAMP signal, that is, they move toward a cAMP signal (chemotacsis). In addition, cells have the mechanism relaying a cAMP signal. Thus, particular surrounding cells aggregate to the core cells, which initially secrete a cAMP signal, as they relay a cAMP signal. Figure 1 shows the schematic representation of chemotactic cell movement caused by a travelling cAMP signal wave. Note that the direction of chemotactic cell movement is opposite to that of a cAMP travelling wave. The slime mold self-organizes spatial patterns such as a target pattern and a spiral pattern in cell density distribution. As time proceeds in the cell aggregation process, circular and spiral patterns in cell density distribution become unstable, that is, their propagating wave fronts break down and another type of a branching pattern so-called "streaming pattern" is organized. After that, at the core of aggregate cells a multi-cellular mound is formed and it becomes a multi-cellular moving slug in the animal stage. Last, a fruiting body is organized. From the fruiting body, many spores spread and they become to vegetative cells. That is, the life cycle returns to the initial vegetative stage.

In this manuscript, focusing on the aggregation process, we explore the mechanism of breakdown of

circular and spiral patterns and a streaming pattern formation process through numerical experiments with a typical previous model. In addition, a simplified model to organize a streaming pattern is proposed to understand essential mechanism of a streaming pattern formation process.

2. Previous Models

Several models simulating the chemotactic pattern formation process observed in the aggregation process have been proposed. The following set of equations is a typical model proposed by Höfer *et al.* (1995),

$$\begin{aligned}\frac{\partial u}{\partial t} &= \Delta u + \sigma\left[\phi(n)\left(bv + v^2\right)\frac{a+u^2}{1+u^2} - \varphi(n)u\right],\\ \frac{\partial v}{\partial t} &= -k_+ uv + k_-(1-v),\\ \frac{\partial n}{\partial t} &= \nabla\cdot\left[\mu(n)\nabla n - \chi(v)n\nabla u\right],\end{aligned} \tag{1}$$

and,

$$\phi(n) = \frac{n}{1-\kappa_\phi n/(K+n)},\quad \varphi(n) = d_1 + d_2\frac{n}{1-\kappa_\varphi n/(K+n)}, \tag{2}$$

$$\mu(n) = \mu_1 + \mu_2\frac{M^r}{M^r+n^r},\quad \chi(v) = \chi_0\frac{v^m}{A^m+v^m}, \tag{3}$$

where u is the concentration of a cAMP signal, v is the fraction of active cAMP receptors per cell and n is cell density. The variables u and v respectively correspond to activator and inhibitor variables in a reaction-diffusion mechanism. Refer to Table 1 for parameter names and their typical values. The first two equations in Eq.(1) are derived from the Martial and Goldbeter model (Martiel and Goldbeter, 1987; Tyson *et al.* 1989). Figure 2 shows the null-clines for the first two equations in Eq.(1). The last equation in Eq.(1) describes temporal evolution of cell density, where the first term in the right side describes cell diffusion and the second term does chemotactic cell movement caused by spatial gradient of a cAMP signal. The functions $\mu(n)$ and $\chi(v)$ are step functions, threshold values of which are denoted by the parameters M and

A, respectively. The function $\mu(n)$ refers to cell-cell adhesion at high cell density. The function $\chi(v)$ has the effect suppressing chemotactic cell movement within the wave back of a cAMP signal. The effect solves so-called "chemotactic wave paradox" (refer to the section 4. for more detail).

A pattern formation process obtained by the model consisting of Eqs.(1)-(3) shows the good agreement with that observed in real laboratory experiments. Figure 3 shows the result of a 1-dimensional numerical experiment obtained by the model consisting of Eqs.(1)-(3). The left side of the system was triggered for the u component at the initial condition. Then, a set of waves on u, v and n was organized at the triggered left side. Since total cell density is conserved, cells were piled at the left side. The set of waves was propagating from left to right at constant velocity. The propagating wave having low cell density region refers to chemotactic cell movement. While the direction of the propagating wave is left to right, the direction of the chemotactic cell movement is right to left, that is, opposite to that of the wave propagation. In addition, the movement is caused only within passage of the cAMP signal wave front. Figure 4 shows result of a 2-dimensional numerical experiment with the model consisting of Eqs.(1)-(3). Initially 6 positions were triggered for the u component under cell density distribution perturbed with small noise n=1.0±0.1. In the initial stage, 4 groups of spiral waves were survived. When cell density became high at the spiral cores (Fig.4(b)), pitch of wave trains became narrow (Fig.4(a)) and their propagating speed became high. Then, the spirals were becoming unstable. Last, wave fronts around the cores of the spiral waves broke down (Fig.4(c)) and streaming patterns were organized in the cell density distribution (Fig.4(d)).

Höfer and Maini (1997) proposed the following minimal model simulating the aggregation process,

$$\begin{aligned} \frac{\partial u}{\partial t} &= \Delta u + \sigma(n) f(u,v), \\ \frac{\partial v}{\partial t} &= g(u,v), \\ \frac{\partial n}{\partial t} &= \mu \Delta n - \nabla \cdot [\chi(v) n \nabla u], \end{aligned} \qquad (4)$$

where $f(u,v)$ and $g(u,v)$ are reaction terms (refer to Fig 5 for their null-clines), $\sigma(n)$ is an increasing function of n, μ is a constant parameter and $\chi(v)$ is an increasing function of v. Equation (4) consists of 2 parts, one of which is a reaction-diffusion mechanism with a function $\sigma(n)$ controlling reaction speed and the other of which is a cell density evolution equation describing a cell diffusion and a chemotactic cell movement caused by spatial gradient of an activator variable u with the function $\chi(v)$ solving "chemotactic wave paradox". Other previous models proposed by other researchers are in the same form (Vasiev *et al.* 1994; Polzehaev *et al.* 1998).

3. Mechanism of Streaming Pattern Formation

In this section the mechanism of a streaming pattern formation process is explored through numerical experiments. Our main questions are why circular and spiral waves break down and why a streaming pattern is organized. Previous studies did not clearly state the mechanism.

The following 2-dimensional numerical experiment provides us with the key information to understand the mechanism of the streaming pattern formation process (Fig.6). First, the 1-dimensional wave train was generated with the model consisting of Eqs.(1)-(3). Next, the 1-dimensional wave train was arranged vertically in a 2-dimensional domain, where small rectangular perturbation for the n component was set in the domain. The wave train simulates spiral waves or multi-triggered circular waves without their curvature effect. Finally, a numerical calculation with the 2-dimensional version of the model was carried out. Figure 6 shows the result of the numerical experiment. When a wave travels on the perturbed region, it enlarges the original perturbation on cell density n (see Fig.6 and compare the vertical profiles of n obtained at t=0.7 and t=0.8).

The above numerical experimental result shows us the mechanism of the streaming pattern formation process (Fig.7). When a wave reaches the perturbed region having high cell density, part of the wave front

located on the perturbed region travels faster than the other part does, since wave speed is almost proportional to cell density n (Fig.8). Difference on traveling wave speed causes wave front deformation (see $u(x,y,t=0.8)$ and $n(x,y,t=0.8)$ in Fig.6). While planar wave front causes chemotactic cell movement whose direction is parallel to that of wave propagation, deformed wave front causes chemotactic cell movement whose direction is not only parallel but also perpendicular to that of wave propagation (Fig.7 (b)). This chemotactic cell movement perpendicular to the wave propagation direction enlarges the original cell density perturbation. Cell density around the initially perturbed region becomes higher than that of the initial cell density (Fig.6(c)); on the other hand, cell density around the neighboring region becomes lower. Since a wave train repeats this mechanism over and over, cell density difference of initial perturbation is becoming larger and larger. The cell density difference travels along with the train wave propagation. This leads to a streaming pattern and breakdown of a wave train.

4. Simplified Models

In order to understand the essential mechanism of a streaming pattern formation process, it is important to derive a simplified model. First, I show that the minimal model Eq.(4) proposed by Höfer and Maini (1997) generates a streaming pattern. The following FitzHugh-Nagumo type equations (FitzHugh, 1961; Nagumo *et al.*, 1962) are utilized as the reaction terms of $f(u,v)$ and $g(u,v)$,

$$\begin{aligned} f(u,v) &= u(u-\alpha)(1-u)-v, \\ g(u,v) &= \beta u - v, \end{aligned} \tag{5}$$

where α and β are constants. The functions $\sigma(n)$ and $\chi(v)$ in Eq.(4) are set to the following linear functions,

$$\begin{aligned} \sigma(n) &= \sigma_0 n, \\ \chi(v) &= \chi_0 (v_0 - v), \end{aligned} \tag{6}$$

where σ_0, χ_0 and v_0 are constants. Figure 9 shows a 1-dimensional wave train and a streaming pattern

formation process obtained by the simplified model consisting of Eqs.(4)-(6). From these results, we can understand that the minimal model reproduces a streaming pattern formation process.

Now, I explain the effect of the function $\chi(v)$ suppressing the chemotactic cell movement within wave back. Let us assume that the chemotactic cell movement is always effective, that is, $\chi(v) = \chi_0$. Then, chemotactic cell movement is caused by concentration gradient of a cAMP signal wave within wave front and also within wave back. However, direction of chemotactic cell movement within wave front is opposite to that within wave back. Thus, it is believed that chemotactic cell movement is cancelled. This is so-called "chemotactic wave paradox". Therefore, to solve the chemotactic wave paradox, all of the previous models including the minimal model of Eq.(4) have the step function $\chi(v)$ suppressing the chemotactic cell movement within wave back.

However, I show that the function $\chi(v)$ solving the chemotactic wave paradox is not necessary to organize a streaming pattern. First, I present a simplified model based on the assumption that $\chi(v)$ is constant. In the minimal model of Eq.(4) I utilize the FitzHugh-Nagumo type equations as reaction terms and the following functions as $\sigma(n)$ and $\chi(v)$,

$$\sigma(n) = \frac{\sigma_0}{n}, \qquad \chi(v) = \chi_0. \tag{7}$$

Figure 10 (a) shows the 1-dimensional wave train obtained by the simplified model consisting of Eqs.(4), (5) and (7). Chemotactic cell movement is observed within wave front and within wave back. The profile of the chemotactic cell movement is asymmetric and the amount of chemotactic cell movement within the wave back is larger than that within the wave front. Thus, the direction of net chemotactic cell movement is same as that of wave propagation and opposite to the direction of chemotactic cell movement observed in the previous models. This implies that the function $\sigma(n)$ should be inversely proportional to cell density n under the fixed χ_0 for organizing a streaming pattern as shown in Fig.11. Using the 1-dimensioanl result

of a wave train (Fig.10(a)), I carried out a 2-dimensional numerical experiment. Then, I successfully realized a streaming pattern formation process as shown in Figure 10(b).

5. Conclusion

In this manuscript, I have reviewed the previous models describing breakdown of spiral and target patterns and a streaming pattern formation process on the aggregation process of the *Dictyostelium* discoideum. Through several numerical experiments with one of the previous models, I have shown the mechanism why spiral and target patterns break down and why such a streaming pattern is organized. In addition, a simplified model based on the model proposed by Höfer and Maini (1997) has been proposed. The simplified model does not take account of so-called "chemotactic wave paradox" for more simplification. I have shown that the simplified model can organize a streaming pattern in spite of the simplification.

Acknowledgements

The author would like to thank Prof. Mimura (Hiroshima University) for his valuable suggestions and discussions. Part of this study was completed while the author was visiting the Faculty of Science, Hiroshima University.

References

FitzHugh, R. (1961) Impulses and physiological states in theoretical models of nerve membrane, *Biophysical Journal* **1**, pp.445-466.

Höfer, T., J. A. Sherratt and P. K. Maini (1995) Cellular pattern formation during *Dictyostelium* aggregation, *Physica D* **85**, pp.425-444.

Höfer, T. and P. K. Maini (1997) Streaming instability of slime mold amoebae: An analytical model, *Physi-*

cal Review E **56**, pp.2074-2080.

Martiel, J.-J. and A. Goldbeter (1987) A model based on receptor desensitization for cyclic AMP signaling in *Dictyostelium* cells, *Biophysical Journal* **52**, pp.807-828.

Nagumo, J., S. Arimoto and S. Yoshizawa (1962) An active pulse transmission line simulating nerve axon, *Proceedings of the IRE* **50**, pp.2061-2070.

Polezhaev, A. A., V. S. Zykov and S. C. Müller (1998) Destabilization of cell aggregation under nonstationary conditions, *Physical Review E* **58**, pp.6328-6332.

Tyson, J. J., K. A. Alexander, V. S. Manoranjan and J. D. Murray (1989) Spiral waves of cyclic AMP in a model of slime mold aggregation, *Physica D* **34**, pp.193-208.

Vasiev, B. N., P. Hogeweg and A. V. Panfilov (1994) Simulation of *Dictyostelium Discoideum* aggregation via reaction-diffusion model, *Physical Review Letters* **73**, pp.3173-3176.

Table 1. Typical parameter values utilized in the previous model consisting of Eqs.(1)-(3).

Name	σ	a	b	d_1	d_2	k_+	k_-	χ_0
Value	70.0	0.014	0.2	0.026	0.234	2.5	2.5	0.5
Name	μ_1	μ_2	A	M	K	$\kappa_\phi, \kappa_\varphi$	m	r
Value	0.003	0.0095	0.72	1.2	8.0	0.7	10.0	4.0

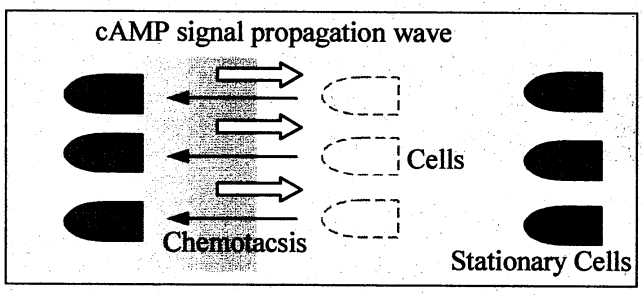

Fig.1 Propagation of a cAMP signal wave and its chemotactic cell movement (chemotacsis).

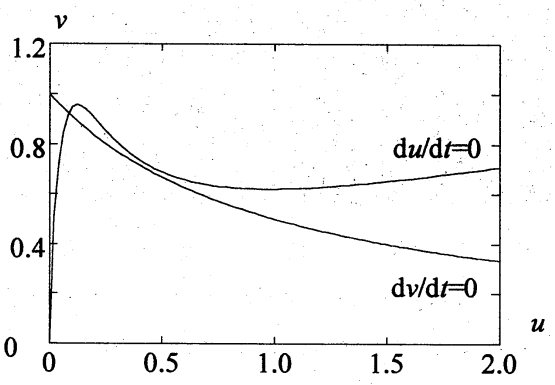

Fig.2 Null-clines for the model Eq.(1) with Eqs.(2) and (3). Cell density n is fixed to 1.0. Refer to Table 1 for parameter values.

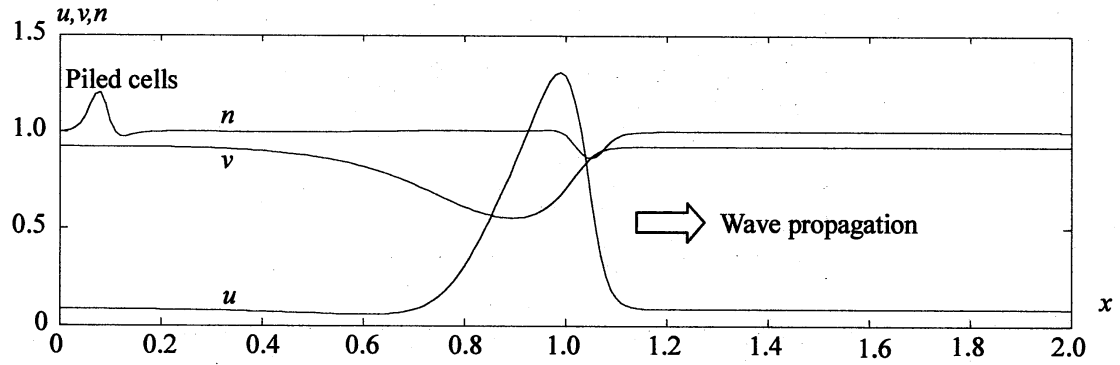

Fig.3 Numerical experiment with the model consisting of Eqs.(1)-(3) at t=2.0. A cAMP wave propagates from left to right. Refer to Table 1 for parameter values utilized in this experiment. Boundaries are defined by the Neumann zero condition for the both sides.

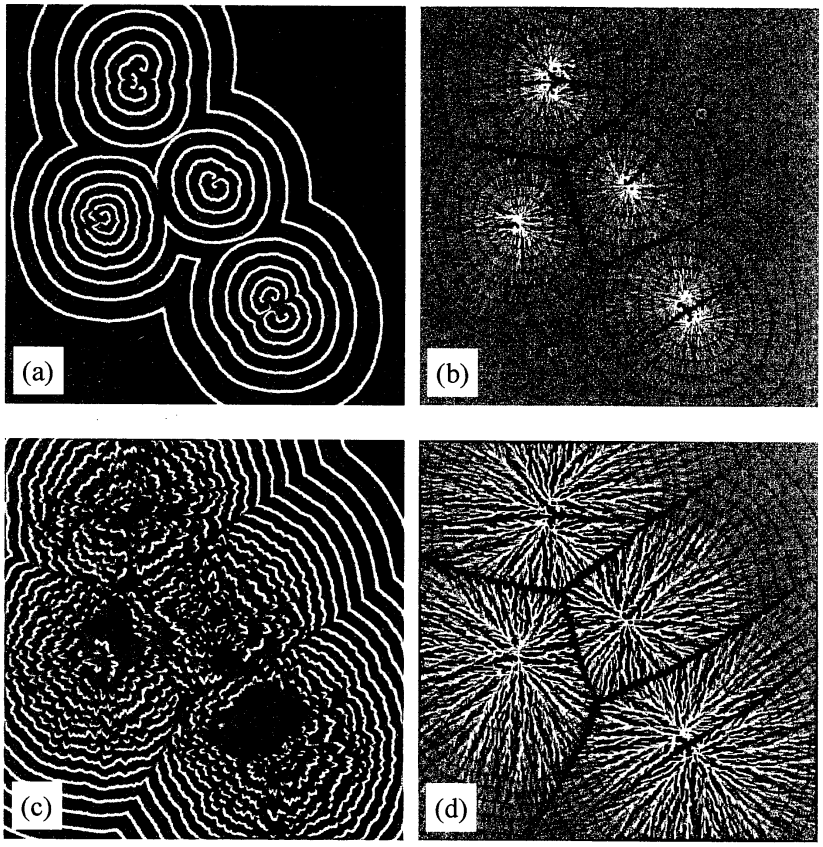

Fig.4 Numerical experiment with the model consisting of Eqs.(1)-(3) in a 2-dimensional domain System size is 400×400 (mesh). (a) $u(x,y,t=15)$, (b) $n(x,y,t=15)$, (c) $u(x,y,t=30)$ and (d) $n(x,y,t=30)$. Refer to Table 1 for parameter values utilized in this experiment. Boundaries are defined by the Neumann zero condition for the four sides.

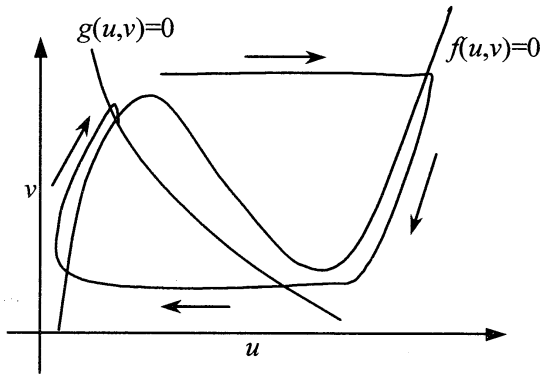

Fig.5 Null-clines for a typical FitzHugh-Nagumo type reaction model utilized in the simplified model of Eq.(4).

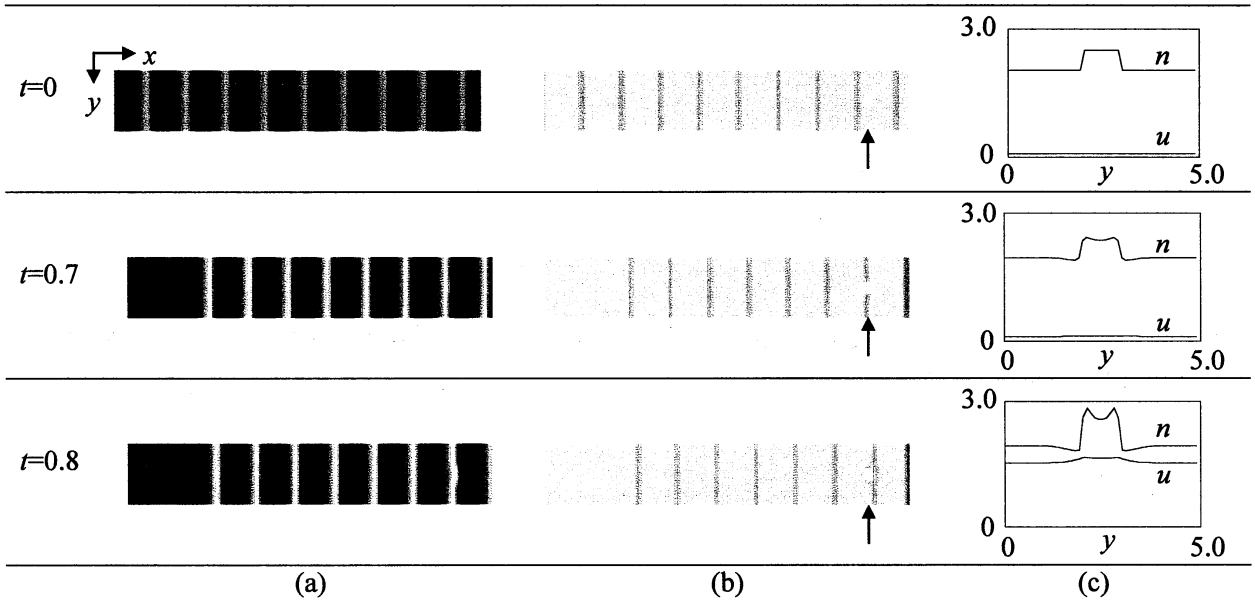

Fig.6 Numerical experiment of a 2-dimensional wave train with the model consisting of Eqs.(1)-(3). (a) $u(x,y,t)$, (b) $n(x,y,t)$ and (c) 1-dimensional vertical profiles at the horizontal position indicated with the arrows in (b). Refer to Table 1 for parameter values utilized in this experiment. System size is 300×50 (mesh).

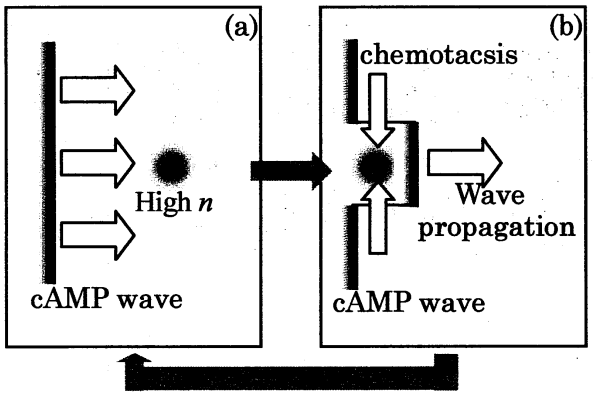

Fig.7 Schematic representation of a streaming pattern formation process. When a planar wave reaches the high cell density region (a), the planar wave is deformed by the dependence of wave speed on cell density (Fig.8). The wave front deformation causes the chemotactic cell movement perpendicular to the direction of the wave propagation (b).

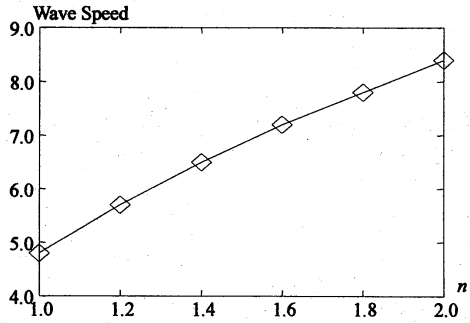

Fig.8 Dependence of wave propagation speed on initial cell density n. The model consisting of Eqs.(1)-(3) is utilized. Refer to Table 1 for parameter values.

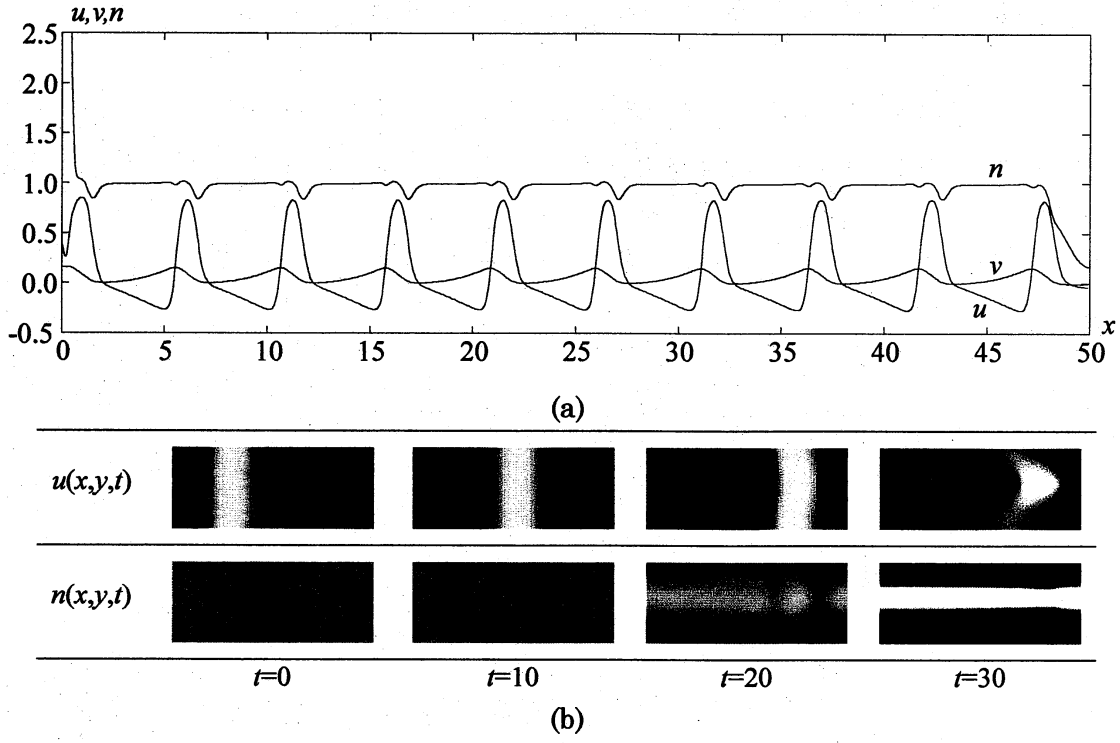

Fig.9 Numerical experiments of a 1-dimensional wave train (a) and a streaming pattern formation process (b) obtained by the simplified model consisting of Eqs.(4)-(6). Parameter values utilized in these experiments are $\alpha = 0.05$, $\beta = 1.0$, $\sigma_0 = 100$, $\chi_0 = 5.0$, $v_0 = 0.14$ and $\mu = 0.01$. Boundaries are defined by the Neumann zero condition for the 1-dimensional experiment and by the periodic condition for the 2-dimensional experiment. System size of the 2-dimensional domain is 100×40 (mesh).

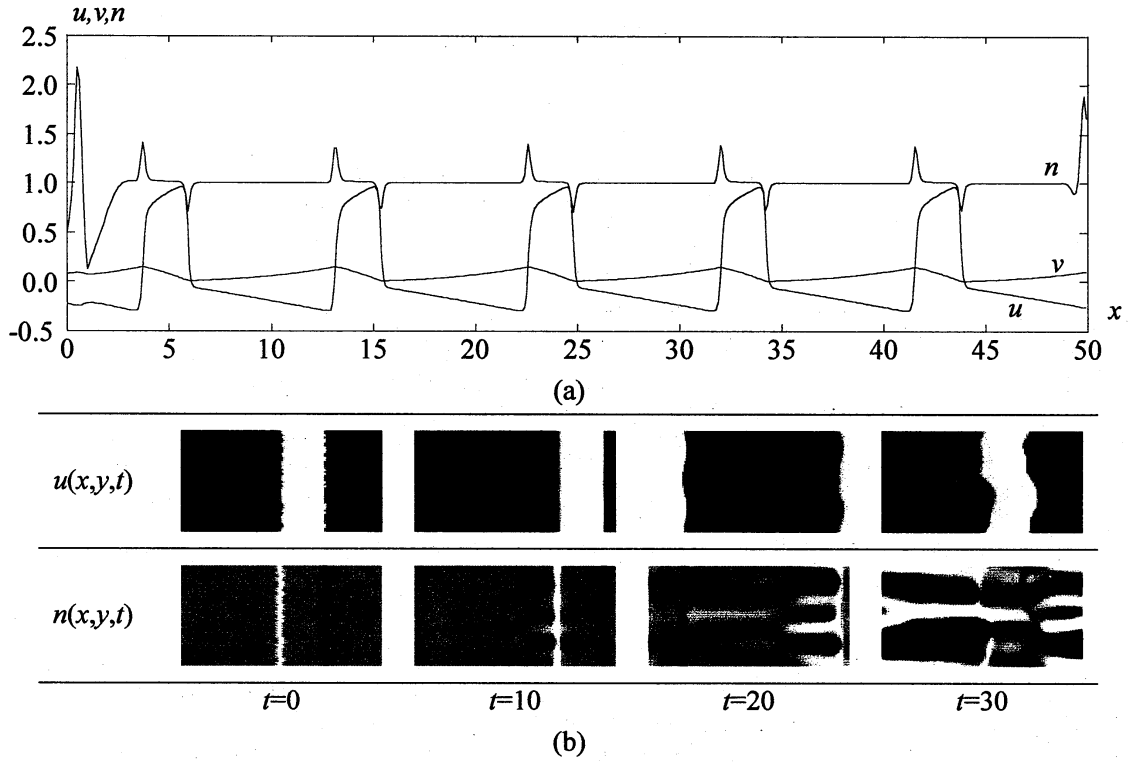

Fig.10 Numerical experiments of a 1-dimensional wave train (a) and a streaming pattern formation process (b) obtained by the simplified model consisting of Eqs.(4), (5) and (7). In the 1-dimensional wave train, net chemotactic cell movement is from left to right (focus on the right side and the left side in the 1-dimensional domain). Parameter values utilized in these experiments are $\alpha = 0.05$, $\beta = 1.0$, $\sigma_0 = 500$, $\chi_0 = 1.0$ and $\mu = 0.01$. Boundaries are defined by the Neumann zero condition for the 1-dimensional experiment and by the periodic condition for the 2-dimensional experiment. System size of the 2-dimensional domain is 100×50 (mesh).

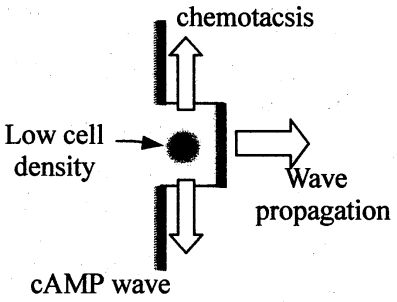

Fig.11 Chemotactic cell movement in the simplified model consisting of Eqs.(4), (5) and (7). The function $\sigma(n) = \sigma_0 / n$ makes the part of the wave around the low cell density region faster than other part. Chemotactic cell movement perpendicular to the direction of the wave propagation is directed from low cell density region to high cell density region. Thus, initial perturbation on cell density is enlarged by the passage of the wave.